

# BASIC BIOMECHANICAL CHARACTERIZATION OF POLYURETHANE BASED ARTIFICIAL CANCELLOUS STRUCTURES

JAN ŠLEICHT<sup>a,b,\*</sup>, DANIEL KYTÝŘ<sup>a</sup>, KATEŘINA PITHARTOVÁ<sup>a,b</sup>,  
SASCHA SENCK<sup>c</sup>, DAVID FÜRST<sup>d</sup>, ANDREAS SCHREMPF<sup>d</sup>

<sup>a</sup> Czech Academy of Sciences, Institute of Theoretical and Applied Mechanics Prosecká 809/76, 190 00 Prague 9, Czech Republic

<sup>b</sup> Czech Technical University in Prague, Faculty of Transportation Sciences, Konviktská 20, 110 00 Prague 1, Czech Republic

<sup>c</sup> University of Applied Sciences Upper Austria in Wels, Computed Tomography Research Group, Stelzhamerstrasse 23, 4600 Wels, Austria

<sup>d</sup> University of Applied Sciences Upper Austria in Linz, Research Group for Surgical Simulators Linz, Garnisonstrasse 21, 4020 Linz, Austria

\* corresponding author: [sleichrt@itam.cas.cz](mailto:sleichrt@itam.cas.cz)

**ABSTRACT.** The main goal of this study is to validate elementary mechanical parameters of a newly designed open-cell foam. The purpose for investigating artificial material is to approach the properties of the human bone in the case of its adequate replacement. Investigated material can be also used as an artificial bone to train surgical procedures and to improve the skills of the surgeons. Four sets of the foam with different chemical composition were subjected to an uniaxial quasi-static loading to describe basic mechanical behaviour of these samples. Based on these experiments, the stress-strain diagrams were created as a comparative tool including calculation of the effective Young's modulus. The acquired knowledges will be used as input parameters of a follow-up study aimed at describing the morphology of presented structures and their response to mechanical experiments. A distortion effect of porosity on the results is not considered in this study.

**KEYWORDS:** polyurethane foam, artificial bone, uniaxial loading, digital image correlation.

## 1. INTRODUCTION

Open cell foams are very effective lightweight structures with impressive load-bearing function. Therefore there is wide range of application for this type of material in modern engineered products. Moreover, this spongy-like structure is very close to natural foam materials hence it meets the presumption for the usage in bioengineering [1]. In this case different types of polyurethane foam synthesized as artificial cancellous bone was investigated from biomechanical point of view.

The goal of the project is to find suitable material for artificial vertebrae filling with similar mechanical and structural parameters to real vertebra body [2]. Resulting product will serve during the training of medical doctors in spine surgery simulator developed at FHOÖ Linz [3].

Based on results of previous studies [4], four different foam were synthesized employing various additives in base polyurethane matter. Similarly to the natural cancellous bone, artificial structure exhibit complex porous microstructure composed of irregular polyhedral cells [5] which is influenced by the additives. Bone aging and disease could be simulated the same way [6, 7]. Set of pilot compression tests were performed on batch of samples prepared from all ma-

terial to evaluate basic mechanical parameters and to test loading range for in-house developed loading device which is planned to be used for 4D computed tomography testing procedure as a next step in this project.

## 2. EXPERIMENTAL PROCEDURE

### 2.1. SPECIMEN DESCRIPTION

Two-component polyurethane resin (Kaupo, Spaichingen, Germany) was used as the base material. Depending on a mineral filler, four types of polyurethane foam were created (listed in Tab. 1). Each type of foam was provided by the Research Group for Surgical Simulators Linz (University of Applied Sciences Upper Austria in Linz, Austria). A small amount of highly-concentrated colour pigments was added to distinguish individual sets of samples (depicted in Fig. 1). The same additives (in detail listed in [4]) were used in all cases, e.g. 1% of tap water as a blowing agent.

All the foam samples were delivered in cylindrical shape with thin outer shell and cut by a band saw to smaller rollers with a diameter  $D = 19.70 \pm 0.14$  mm and height  $h = 15.42 \pm 0.42$  mm.

Filler	Bulk Density [g/dm <sup>3</sup> ]
50% Calcium carbonate (CaCO <sub>3</sub> ) 1% H <sub>2</sub> O 3% stabilizer	416.69 ± 21.85
50% Calcium phosphate (3Ca <sub>3</sub> (PO <sub>4</sub> )·CaO) 1% H <sub>2</sub> O 3% stabilizer	362.15 ± 17.16
30% Barium sulphate (BaSO <sub>4</sub> ) 1% H <sub>2</sub> O 3% stabilizer	381.45 ± 36.07
without filler 1% H <sub>2</sub> O 3% stabilizer	467.33 ± 59.74

TABLE 1. Average bulk density of the samples



FIGURE 1. Four types of samples – color-coded according to the filler

## 2.2. EXPERIMENTAL SETUP

Experimental setup consisted of an in-house developed uni-axial loading device and optical setup. Force was measured by high-durability U9B series loadcell with nominal loading capacity 1 kN (HBM, Germany). The axial movement of a clamp was performed by an electrical stepper motor with a ball screw. Displacement-driven tests were performed with 10 μm/s loading rate for 10 mm displacement (corresponding to ≈ 50% deformation). Force and displacement data were recorded at a sample rate of 5 Hz. Experiments were controlled by the modified LinuxCNC software running on a real-time kernel [8].

Because of the need to evaluate the deformation optically, the samples were captured by high-resolution CCD camera Manta G-504BManta (Allied Vision Technologies GmbH) equipped with a telecentric lens. The optical setup was placed on a 3-axis stage equipped with micrometric screws for precise positioning. All of the images were captured by unique timestamp to synchronize the force log. During the measurement, place of view had to be enlightened by external LED light source KL 2500 (Shott, Germany). Complete equipment is depicted in Fig. 2.

## 2.3. DIGITAL IMAGE CORRELATION

High precision of the deformation measurement is a necessary step for proper evaluation of the strain-stress diagram. One of the common and widely used method is Digital Correlation Image (DIC). This opti-

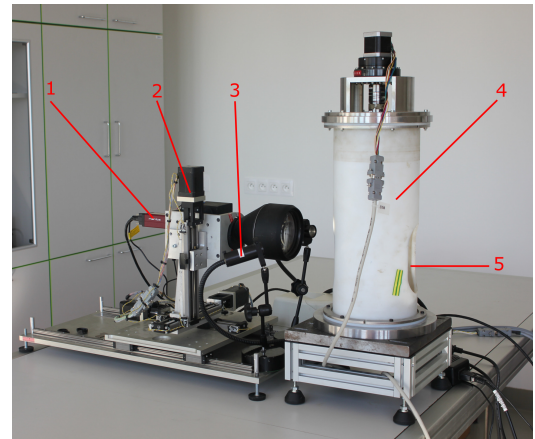


FIGURE 2. 1 - camera, 2 - positionable table, 3 - LED source, 4 - loading device, 5 - place for specimen

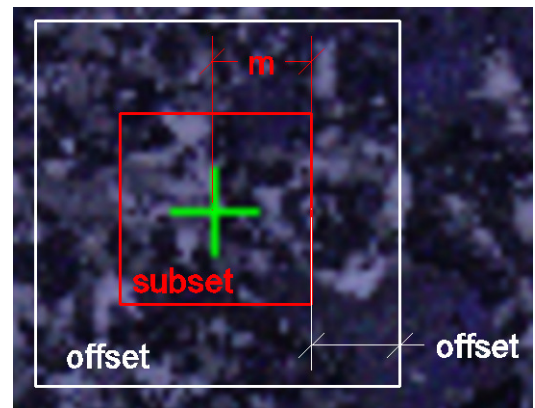


FIGURE 3. Definition of the subset and offset

cal method is based on a specific small area tracking - *subset*, defined by a variable  $m$ . The region is then searched for in the wider neighborhood defined by a variable *offset* (shown in Fig. 3).

A necessary condition is to ensure a granular coating on the surface of each sample. Primarily random pattern allows a tracking of these areas during the experiment and calculation of the displacement, necessary to calculate the deformation. Updated Lucas-Kanade algorithm was used for this purpose [9, 10].

## 3. RESULTS

Based on the obtained force-displacement results, the stress-strain curves were calculated using total dimensions of the samples (Fig. 4 to 7). These results show dependency of the ultimate stress on the used filler in polyurethane foam. The stress-strain curves are very similar when using Calcium phosphate and Barium sulphate filler. Higher values of the monitored quantities are reached by the Calcium carbonate filler. The highest values of the ultimate-stress and Young's modulus are achieved when no filler is used but these results are distorted by a thin shell of a high stiffness on the samples.

Young's modulus was calculated using linear regression applied on the elastic part of the stress-strain

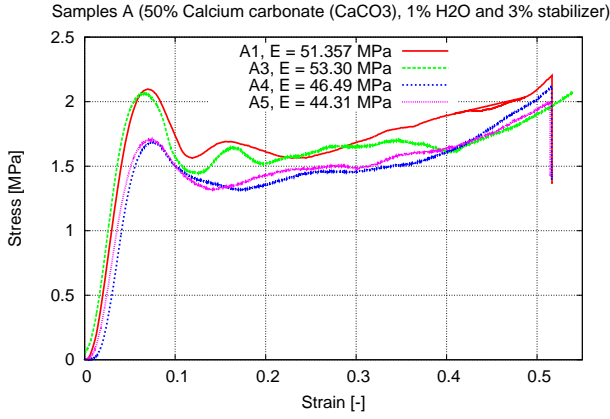


FIGURE 4. Stress-strain curves of Calcium carbonate filler

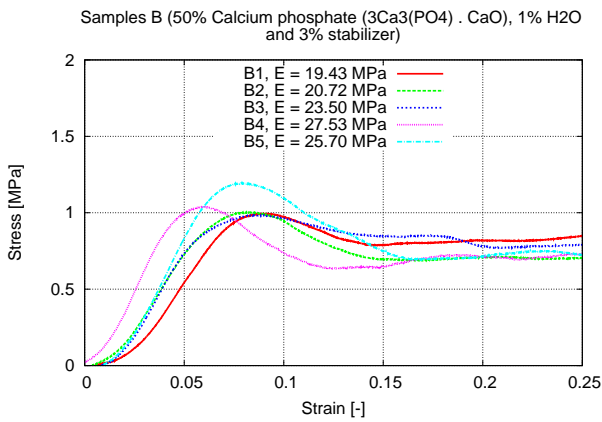


FIGURE 5. Stress-strain curves of Calcium phosphate filler

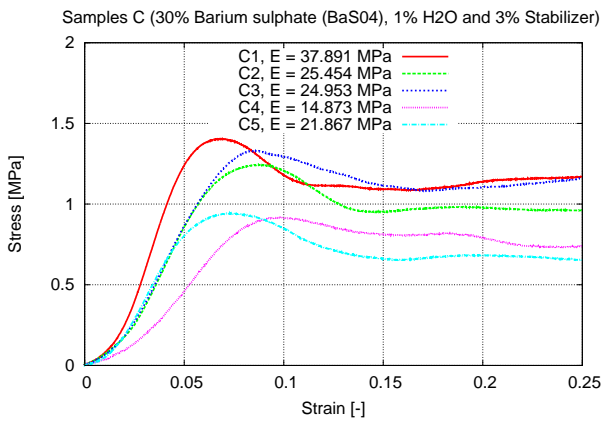


FIGURE 6. Stress-strain curves of Barium sulphate filler

diagrams. For the yield stress  $\sigma_Y$  evaluation, Christensen [11] second derivation criteria was used:

$$\sigma_Y = \sigma \text{ at } \left| \frac{d^2\sigma}{d\epsilon^2} \right| = \max \quad (1)$$

For noise reduction significantly distorting resulting derived function rolling average filter computed from

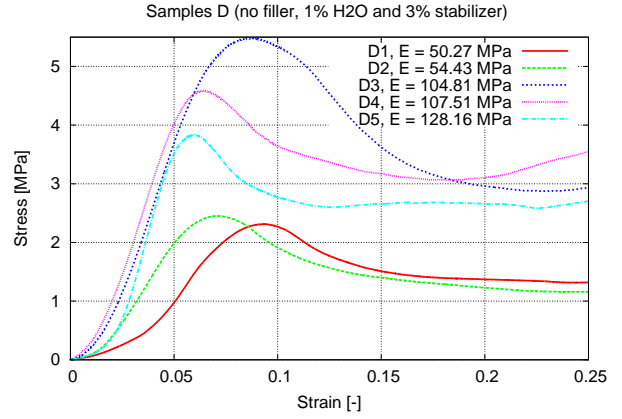


FIGURE 7. Stress-strain curves of no filler

five values as:

$$\sigma'_{n_a} = \frac{\sigma'_{n-2} + \sigma'_{n-1} + \sigma'_n + \sigma'_{n+1} + \sigma'_{n+2}}{5} \quad (2)$$

Results of the effective Young's modulus of each of the sample's batch are listed in Tab. 2.

Filler	Effective Young's modulus [MPa]
50% Calcium carbonate ( $\text{CaCO}_3$ ) 1% $\text{H}_2\text{O}$ 3% stabilizer	$48.63 \pm 4.37$
50% Calcium phosphate ( $3\text{Ca}_3(\text{PO}_4) \cdot \text{CaO}$ ) 1% $\text{H}_2\text{O}$ 3% stabilizer	$23.35 \pm 3.89$
30% Barium sulphate ( $\text{BaSO}_4$ ) 1% $\text{H}_2\text{O}$ 3% stabilizer	$25.01 \pm 8.35$
without filler 1% $\text{H}_2\text{O}$ 3% stabilizer	$89.04 \pm 34.72$

TABLE 2. Average of the effective Young's modulus of the samples

#### 4. CONCLUSIONS

All samples were subjected to the uniaxial compression test. Digital Image Correlation method was used for evaluating the displacement during the measuring. Due to very precise synchronization between captured images of the sample's surface and force logs the stress-strain diagrams could be calculated and effective Young's modulus was calculated for each of the sample. High dispersion of the Young's modulus is described by the standard deviation. This indicates that the porosity or wall thickness vary in the volume of the sample. Further investigation of the material, especially from morphological point of view, is necessary. For this reason, other samples

will be subjected to an internal structure study using more advanced methods as 4D computed tomography testing procedure.

#### ACKNOWLEDGEMENTS

The research has been supported by Operational Programme Research, Development and Education in project Competitiveness Boost of the Centre of Excellence in Vysočina Region (CZ.02.2.69/0.0/0.0/16\_027/0008475), by European Regional Development Fund in frame of the project Com3D-XCT (ATCZ38) in the Interreg V-A Austria - Czech Republic programme and by institutional support RVO: 68378297.

#### REFERENCES

- [1] K. L. Calvert, K. P. Trumble, T. J. Webster, L. A. Kirkpatrick. Characterization of commercial rigid polyurethane foams used as bone analogs for implant testing. *Journal of Materials Science: Materials in Medicine* **21**(5):1453–1461, 2010. DOI:10.1007/s10856-010-4024-6.
- [2] T. Fila, D. Kytýr, P. Zlamal, et al. High-resolution time-lapse tomography of rat vertebrae during compressive loading: Deformation response analysis. *Journal of Instrumentation* **9**(5), 2014. DOI:10.1088/1748-0221/9/05/C05054.
- [3] B. Esterer, J. Razenbock, M. Hollensteiner, et al. Development of artificial tissue-like structures for a hybrid epidural anesthesia simulator. *2016 38th Annual International Conference of the IEEE Engineering in Medicine and Biology Society (EMBC)* pp. 2099–2102, 2016. DOI:10.1109/EMBC.2016.7591142.
- [4] D. Fuerst, S. Senck, M. Hollensteiner, et al. Characterization of synthetic foam structures used to manufacture artificial vertebral trabecular bone. *Materials Science and Engineering C* 2017.
- [5] M. S. Thompson, I. D. McCarthy, L. Lidgren, L. Ryd. Compressive and shear properties of commercially available polyurethane foams. *J Biomech Eng* **125**(5):732–734, 2003. DOI:10.1115/1.1614820.
- [6] H. Chen, S. Shoumura, S. Emura, Y. Bunai. Regional variations of vertebral trabecular bone microstructure with age and gender. *Osteoporosis International* **19**(10):1473–1483, 2008. DOI:10.1007/s00198-008-0593-3.
- [7] H. Chen, X. Zhou, H. Fujita, et al. Age-related changes in trabecular and cortical bone microstructure. *International Journal of Endocrinology* (ID 213234):9, 2013. DOI:10.1155/2013/213234.
- [8] V. Rada, T. Fila, P. Zlamal, et al. Multi-channel control system for in-situ laboratory loading devices. *Acta Polytechnica CTU Proceedings 18:15–19* 2018. DOI:10.14311/APP.2018.18.0015.
- [9] B. Lucas, T. Kanade. An iterative image registration technique with an application to stereo vision. *Proceedings of the 7th international joint conference on Artificial intelligence* **2**:674–679, 1981.
- [10] I. Jandejsek, J. Valach, D. Vavrik. Optimization and Calibration of Digital Image Correlation method. *Proceedings EAN 2010* pp. 121–126, 2010.
- [11] R. M. Christensen. Observations on the definition of yield stress. *Acta Mechanica* **196**(3):239–244, 2008. DOI:10.1007/s00707-007-0478-0.